

Enzyme Replacement Improves Ataxic Gait and Central Nervous System Histopathology in a Mouse Model of Metachromatic Leukodystrophy

Ulrich Matzner¹, Renate Lüllmann-Rauch², Stijn Stroobants³, Claes Andersson⁴, Cecilia Weigelt⁴, Carl Eistrup⁵, Jens Fogh⁵, Rudi D'Hooge³ and Volkmar Gieselmann¹

¹Institut für Physiologische Chemie, Rheinische Friedrich-Wilhelms-Universität, Bonn, Germany; ²Anatomisches Institut, Christian-Albrechts-Universität, Kiel, Germany; ³Laboratory of Biological Psychology, Department of Psychology, University of Leuven, Leuven, Belgium; ⁴Zymenex A/S, Dalenum 13, Lidingö, Sweden; ⁵Zymenex A/S, Roskildevej 12C, Hillerød, Denmark

Inherited deficiencies of lysosomal hydrolases cause lysosomal storage diseases (LSDs) that are characterized by a progressive multisystemic pathology and premature death. Repeated intravenous injection of the active counterpart of the deficient enzyme, a treatment strategy called enzyme replacement therapy (ERT), evolved as a clinical option for several LSDs without central nervous system (CNS) involvement. To assess the efficacy of long-term ERT in metachromatic leukodystrophy (MLD), an LSD with prevailing nervous system disease, we treated immunotolerant arylsulfatase A (ASA) knockout mice with 52 doses of either 4 or 50 mg/kg recombinant human ASA (rhASA). ERT was tolerated without side effects and improved disease manifestations in a dose-dependent manner. Dosing of 4 mg/kg diminished sulfatide storage in kidney and peripheral nervous system (PNS) but not the CNS, whereas treatment with 50 mg/kg was also effective in the CNS in reducing storage in brain and spinal cord by 34 and 45%, respectively. Histological analyses revealed regional differences in sulfatide clearance. While 70% less storage profiles were detectable, for example, in the hippocampal fimbria, the histopathology of the brain stem was unchanged. Both enzyme doses normalized the ataxic gait of ASA knockout mice, demonstrating prevention of nervous system dysfunctions that dominate early stages of MLD.

Received 12 November 2008; accepted 18 December 2008; published online 27 January 2009. doi:10.1038/mt.2008.305

INTRODUCTION

The posttranslational modification of newly synthesized soluble lysosomal enzymes involves the phosphorylation of N-linked oligosaccharide side chains at one or more mannosyl residues.¹ The resulting mannose 6-phosphate (M6P) residues bind to mannose 6-phosphate receptors (MPRs) localized to the trans Golgi network.

This interaction separates lysosomal enzymes from the secretory route and redirects them to the endosomal/lysosomal targeting pathway. MPRs also reside within the plasma membrane where they can bind extracellular ligands exposing M6P recognition markers. As a consequence, exogenous lysosomal enzymes are internalized and transported to the endosomal/lysosomal compartment as well. In case of an absence or inherited functional deficiency of a lysosomal enzyme, a condition leading to a fatal lysosomal storage disease (LSD), this peculiarity of the lysosomal sorting process can be exploited for treatment. The basic treatment concept is to supply the deficient cells with the active counterpart of the mutated enzyme from outside. In enzyme replacement therapy (ERT) this is accomplished by repeated injection of recombinantly expressed enzyme into the circulatory system (for a review see ref. 2). Upon cellular uptake and delivery to the lysosome, the substituted enzyme becomes functionally integrated into the lysosomal degradation pathways, hydrolyzes the accumulated substrate(s), and thereby compensates the catabolic defect.

Preclinical and clinical ERT studies revealed that efficient treatment can be compromised by a variety of factors. These include an immune response to the therapeutic enzyme,^{3,4} the persistence of already established cellular degeneration and organ dysfunctions,^{5,6} inefficient cellular uptake of substituted enzyme,⁷ and a poor accessibility of affected tissues.⁸ In the latter regard, the blood-brain barrier (BBB) is a major issue because it prevents efficient transfer of systemically administered enzyme from the circulation to the brain parenchyma. Due to the low permeability of the BBB for lysosomal enzymes, the central nervous system (CNS) disease that prevails in the majority of LSDs, has been believed to be resistant to ERT.

This view has been challenged by recent preclinical ERT studies demonstrating clearance of CNS storage in mouse models of aspartylglucosaminuria,⁹ α -mannosidosis,^{10,11} and Sly disease.¹² In all three models, ERT led to significant levels of therapeutic enzyme in brain. It is still unclear which parameters favor the transfer of enzyme into the CNS of these animals. ERT also

alleviated CNS storage of an arylsulfatase A (ASA) knockout mouse model of metachromatic leukodystrophy (MLD).¹³ Due to the significant improvement of the nervous system pathology and function, the main site of disease in MLD,¹⁴ ERT was suggested as a viable treatment option for the human disorder. Thus far, the determination of the full therapeutic potential of ERT in mice was, however, prevented by a progressive immune response to the repeatedly injected human enzyme.³ To circumvent this limitation of the conventional ASA knockout mouse, we have recently constructed an immunotolerant ASA knockout mouse line that does not express antibodies to repeatedly injected recombinant human ASA (rhASA) due to lifelong expression of an active site mutant of human ASA from a stably integrated transgene.¹⁵ This study was designed to evaluate the full therapeutic potential of ERT for ASA knockout mice by treating 6–7-week-old immunotolerant ASA knockout mice 2 times a week for 26 weeks (52 injections). To evaluate a possible dose dependency of therapeutic effects, we treated two cohorts of mice: One was treated with a lower enzyme dose (4 mg/kg) and another with a higher dose (50 mg/kg).

RESULTS

Absence of side effects

Six-to-seven-week-old mice (26 per group) were treated for 26 weeks with two weekly bolus injections of either 4 or 50 mg/kg rhASA into the tail vein. Controls were mock treated by injection of buffer. Possible side effects were monitored by visual inspection of cage behavior, food and water consumption, and measurement of body weight. During treatment weeks 13 and 26, hematological parameters (hemoglobin concentration, corpuscular indexes, blood chemistry, coagulation) and urinary parameters (pH, specific gravity, concentration of analytes) were analyzed. After necropsy organs were dissected, weighed, and histologically analyzed. None of the evaluated parameters showed any alteration compared to mock-treated controls (not shown). Most important, hypersensitivity reactions and mortality, which limited the treatment of conventional ASA knockout mice to 4 weeks,¹³ were absent throughout the entire treatment period. Anti-rhASA antibodies were undetectable in all but 2 animals that showed low, but significant titers (not shown), and were excluded from subsequent analyses.

Lipid analysis

Cholesterol, sphingomyelin, and sulfatide levels of kidney, peripheral nerves (plexus brachialis, nervus ischiadicus), spinal cord, and total brain were analyzed by thin layer chromatography (TLC). To quantify sulfatide reduction, ASA knockout mice treated with 4 or 50 mg/kg rhASA were compared with age-matched mock-treated knockout mice and untreated wild-type mice. TLC revealed significant differences in the sulfatide concentrations between mock-treated ASA knockout mice and wild-type controls. Thus, sulfatide levels were increased around 1.4-fold in peripheral nervous system (PNS) and CNS and >15-fold in kidney (Figure 1). Compared to mock treatment with buffer, treatment with 4 mg/kg rhASA reduced excess sulfatide in kidneys of ASA knockout mice by 21% (Figure 1a) and in peripheral nerves by 50 to 62% (Figure 1b,c) on average. In contrast to peripheral tissues, no significant decline was detectable in the CNS (Figure 1d,e).

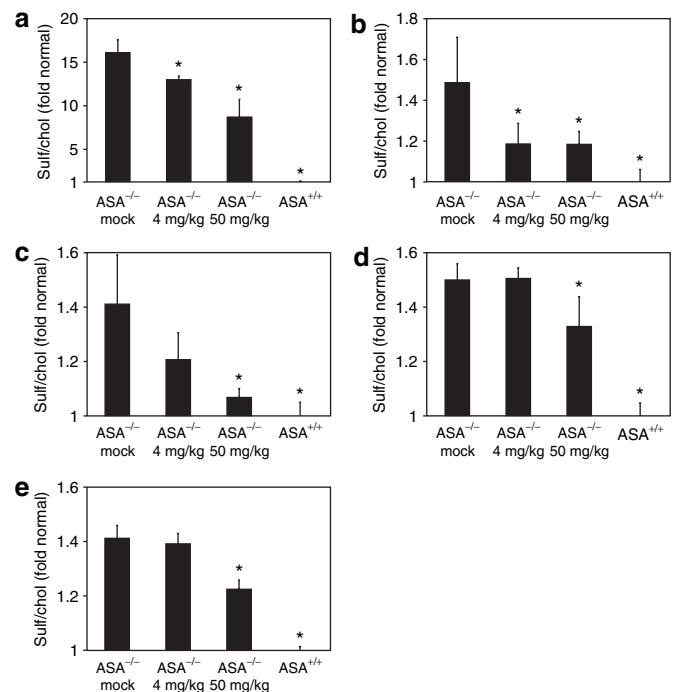


Figure 1 Tissue levels of sulfatide. Lipids were analyzed in (a) kidney, (b) plexus brachialis, (c) sciatic nerve, (d) total brain, and (e) cervical spinal cord. The lipid profiles of the indicated groups of mice were determined by TLC. For a precise quantification of sulfatide (sulf) storage, cholesterol (chol) was used as an internal standard, and the ratio between sulf and chol was calculated. The normalized sulf levels are expressed as fold increase above mean levels of wild-type tissues. Bars represent means \pm SDs ($n = 3$). Statistically significant differences to mock-treated ASA knockout mice are indicated by asterisks ($P < 0.05$). ASA^{-/-}, arylsulfatase A knockout mice; ASA^{+/+}, ASA wild-type control mice.

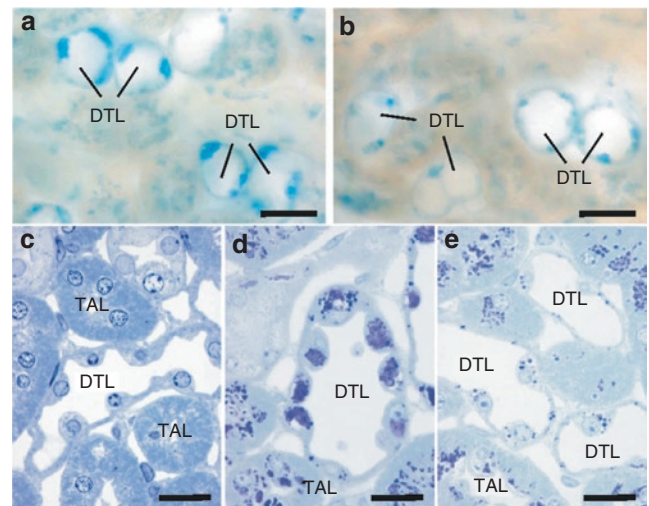


Figure 2 Sulfatide storage in kidney. (a,b) 100 μ m slices through corresponding regions of kidneys from arylsulfatase A (ASA) knockout mice that were either mock treated with buffer (a) or enzyme treated with 50 mg/kg recombinant human ASA (b). Representative examples are shown of descending thin limbs (DTLs) of long loops in the inner stripe of outer medulla. Sulfatide storage material appears blue. (c–e) Semithin sections through DTLs and thick ascending limbs (TALs) stained with toluidine blue that stains storage material dark blue to purple. Corresponding regions of a wild-type control mouse (c), a mock-treated ASA knockout mouse (d), and an ASA knockout mouse treated with 50 mg/kg recombinant human ASA (e) are shown. Bars correspond to 20 μ m.

Treatment with 50 mg/kg rhASA was more effective than low-dose treatment in all tissues under investigation. It diminished excess sulfatide in kidney by 50% (Figure 1a) and in peripheral nerves by 63 to 84% (Figure 1b,c). Most important, the mean sulfatide storage was also significantly reduced in total brain and spinal cord where 34 and 45% of excess sulfatide had disappeared, respectively (Figure 1d,e).

Histological investigations

Sulfatide storage patterns were analyzed in kidney and several parts of the CNS (inner ear, spinal cord, brain stem, hippocampal fimbria) from three ASA knockout mice treated with 50 mg/kg rhASA, three mock-treated ASA knockout mice, and one age-matched wild-type mouse. Wild-type organs showed virtually no alcianophilic structures (shown for kidney in Figure 2c).

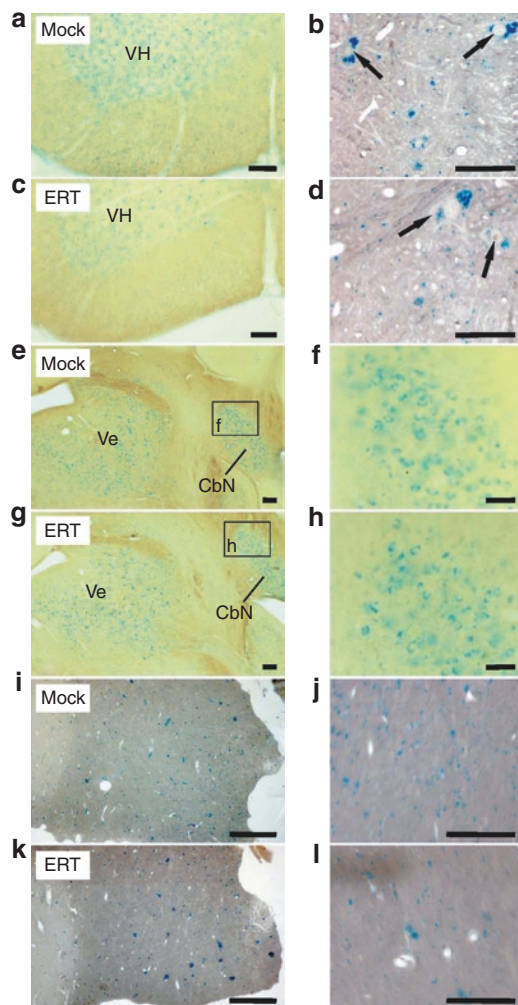


Figure 3 Sulfatide storage in the central nervous system. Corresponding sections from mock-treated arylsulfatase A (ASA) knockout mice (mock) and knockout mice treated with 50 mg/kg recombinant human ASA (ERT) are compared at low (left panel) and high resolution (right panel). Bars correspond to 100 (left panel) and 50 µm (right panel), respectively. (a–d) Spinal cord. 100-µm slices (a,c) and paraffin sections (b,d). The large particles in the gray matter are seen to correspond to sulfatide-storing neuronal perikarya (arrows). (e–h) Brain stem (100-µm slices). The vestibular (Ve) and the lateral cerebellar nucleus (CbN) are positively stained due to sulfatide storage in the neurons as seen at higher resolution. (i–l) Hippocampal fimbria (paraffin sections).

Because TLC had revealed no reduction of sulfatide levels in the CNS of low-dose-treated mice, mice treated with 4 mg/kg were not histologically examined.

In the kidneys of mock-treated ASA knockout mice the distribution of alcianophilic material was the same as described previously¹⁶ with the thick ascending limbs (TALs) and the descending thin limbs of long loops being the most severely affected parts of the nephron. In the enzyme-treated ASA knockout mice a clear reduction of alcianophilic material was observed in the descending thin limb (Figure 2). In the TAL such a reduction was not obvious.

In 100 µm slices from the CNS of the present knockout mice several populations of alcianophilic profiles were observed. The larger ones usually corresponded to sulfatide-storing neuronal perikarya (shown for spinal cord in Figure 3b,d). Large sulfatide-storing microglial cells (phagocytes), which are a regular occurrence in the CNS of 13–24-month-old ASA knockouts,^{13,17} were not seen in the present 7-month-old knockout mice, except for the hippocampal fimbria as described below. The smaller alcianophilic profiles, according to the earlier experience with ASA knockouts, most likely corresponded mainly to oligodendrocytes. In the spinal cord of rhASA-treated knockout mice, the overall density of alcianophilic particles appears to be reduced particularly in the ventral horn and in the white matter (Figure 3a,c). This could be verified by morphometric evaluation, which revealed a significant reduction of the mean number of storage profiles by 22% ($P = 0.011$; Figure 4a). The brain stem was examined at a defined level (Figure 3e–h) comprising the vestibular nuclei, lateral cerebellar nucleus, the intramedullary portion of the facial nerve, and the ventral cochlear nucleus. Alcianophilic material was mainly seen in neuronal perikarya (Figure 3f,h). Enzyme treatment failed to yield an obvious reduction of the storage material. The hippocampal fimbria (Figure 3i–l) is one of the central white matter regions where, according to previous experience, large alcianophilic phagocytes occur already in relatively young ASA knockout mice. Therefore, this portion was investigated in order to test whether or not enzyme treatment had an influence on the sulfatide storage within these cells. In 5 µm paraffin sections, large profiles

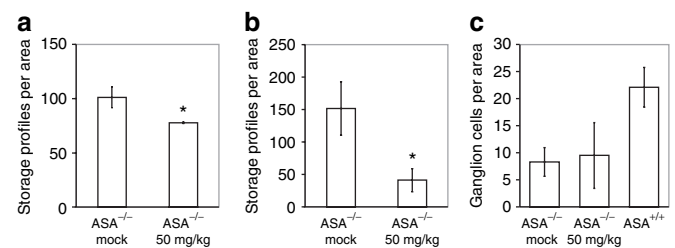


Figure 4 Morphometric analyses of sulfatide storage in the central nervous system of mock-treated arylsulfatase A (ASA) knockout mice (ASA^{-/-} mock), ASA knockout mice treated with 50 mg/kg recombinant human ASA (ASA^{-/-} 50 mg/kg), and wild-type control mice (ASA^{+/+}) are compared. Bars represent means ± SDs. Statistically significant differences between mock- and enzyme-treated ASA knockout mice are indicated by asterisks (for P values see text). (a) Number of alcianophilic profiles in the gray matter of the cervical spinal cord per test area (40,000 µm²), $n = 3$. (b) Number of alcianophilic profiles in the hippocampal fimbria per test area (40,000 µm²), $n = 6$. (c) Number of ganglion cells in the spiral ganglion per test area (10,000 µm²), $n = 3$.

corresponding to sulfatide-storing phagocytes and smaller profiles corresponding to oligodendrocytes were visible (Figure 3i,j). After enzyme treatment the number of large and small alcianophilic particles appeared to be reduced. Morphometric evaluation

confirmed the histological observations by demonstrating 73% less alcianophilic profiles in ERT-treated mice ($P = 0.00006$; Figure 4b). It has to be mentioned that some large profiles typical of phagocytes, albeit significantly reduced in number, were still detectable after treatment (Figure 3l).

In the inner ear of ASA knockout mice the main features are severe sulfatide storage in the perikarya of the spiral and vestibular ganglia and rapid loss of spiral ganglion cells between the 4th and 8th month of life.^{18,19} In this study, the cochleae were examined in 5 μ m paraffin sections (preembedding incubation with alcian blue) and the density of spiral ganglion cells related to the basal turn was evaluated quantitatively. The findings were similar as in previous studies. There was no clear difference between mock- and enzyme-treated mice as far as sulfatide storage and loss of ganglion cells are concerned (Figure 4c).

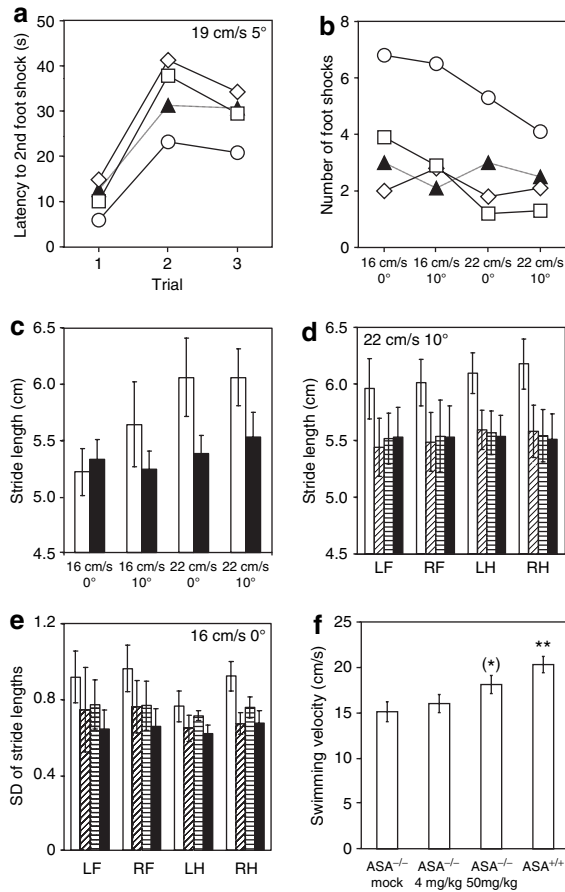


Figure 5 Behavioral analysis of treated mice and controls. (a) Treadmill experiment: latency to the second footshock in the training phase (velocity 19 cm/s, slope 5°). The differences between the experimental groups were not significant. Open circle: mock-treated arylsulfatase A (ASA) knockout mice, open diamond: ASA knockout mice treated with 4 mg/kg recombinant human (rhASA), open square: ASA knockout mice treated with 50 mg/kg rhASA, and closed triangle: wild-type mice. Data points represent means of $n = 6$ animals per group. (b) Treadmill experiment: number of foot shocks in the test phase at different combinations of velocity and slope as indicated (same symbols and group sizes as in a). The statistical analysis revealed significant differences between mock- and enzyme-treated animals (see text). (c) Stride lengths of mock-treated ASA knockout mice (open bars) and wild-type mice (closed bars) measured at different combinations of velocity and slope. For each mouse and condition, the stride lengths of the four paws was averaged. Bars represent means \pm SDs of $n = 6$ mice per group. (d) Stride lengths of individual paws at a treadmill velocity of 22 cm/s and a slope of 10°. LF: left front paw, RF: right front paw, LH: left hind paw, RH: right hind paw, open bar: mock-treated ASA knockout mice, diagonally hatched bars: ASA knockout mice treated with 4 mg/kg rhASA, horizontally hatched bars: ASA knockout mice treated with 50 mg/kg rhASA, and closed bars: wild-type mice. Bars represent means \pm SDs of $n = 6$ mice per group. (e) Standard deviations of the stride lengths measured at a velocity of 16 cm/s and a slope of 0° (same abbreviations, symbols, and group sizes as in d). (f) Mean swimming velocity during 100 s of free swimming. Bars represent means \pm SDs of $n = 6$ mice per group. * $P = 0.05$, ** $P < 0.01$ (compared to mock-treated knockout mice).

Behavioral studies

ASA knockout mice develop progressive motor coordination impairments and ataxia leading to severe behavioral deficits in the second year of life.²⁰⁻²² To determine genotype- and treatment-related effects in the 7-month-old mice of this study, ataxia and other manifestations of motor incoordination were assessed with treadmill and swimming performance tests in immunotolerant ASA knockout mice treated with 4 or 50 mg rhASA/kg, mock-treated knockout mice, and wild-type controls (6 mice per group).

In treadmill experiments mock-treated ASA knockout mice showed impaired gait relative to wild-type mice in all test conditions as indicated by the requirement of earlier or more frequent stimulation (Figure 5a,b). Compared to mock-treated controls, performance of low- and high-dose-treated mice was substantially improved and virtually indistinguishable from the performance of wild-type mice. In the four test trials, for example, mock-treated ASA knockout mice received 5.8-foot shocks on average, whereas 2.2, 2.4, and 2.7 shocks were sufficient for low- and high-dose-treated mice and wild-type controls, respectively (Figure 5b). This indicated a large number of errors in the mock-treated ASA knockouts compared to the other groups. Post hoc analysis revealed significantly improved performance in low- ($P < 0.01$) and high-dose-treated ASA knockout mice ($P < 0.05$) compared to mock-treated ASA knockout mice.

The analysis of the gait pattern revealed increased stride lengths for mock-treated ASA knockout mice, particularly, when they were challenged to walk fast and/or uphill (Figure 5c). Treatment with 4 and 50 mg/kg rhASA led to a normalization

Table 1 Correlation of right to left front/hind distances depending on trial conditions

	ASA ^{-/-}	ASA ^{-/-}	ASA ^{-/-}	ASA ^{+/+}
	Mock	4 mg/kg	50 mg/kg	
16 cm/s and 0° ^a	0.38	0.25	0.83^{ab}	0.91*
16 cm/s and 10°	0.77	0.75	0.85*	0.73
22 cm/s and 0°	0.53	0.65	0.79	0.92**
22 cm/s and 10°	-0.11	0.31	0.60	0.95**

Abbreviations: ASA^{-/-}, arylsulfatase A knockout mouse; ASA^{+/+}, ASA wild-type control.

^aVelocity and slope. ^bValues >0.8 are printed in bold. Asterices indicate significance: * $P < 0.05$, ** $P < 0.01$.

of the mean stride lengths (Figure 5d). However, despite strong trends the differences did not reach statistical significance for any of the four combinations of velocity and slope. When the stride lengths measured under the four conditions were combined, the stride lengths of the right hind paw was significantly reduced ($P < 0.05$).

Also the variation of the stride lengths is increased in mock-treated ASA knockout mice when compared to wild-type controls. In contrast to the absolute stride lengths, the stride lengths variation is, however, highest during horizontal walking at low speed (16 cm/s and 0°). Under these conditions, the mean value for the four paws of mock-treated ASA knockout mice was increased by 38% compared to wild-type controls (Figure 5e). Treatment with 4 or 50 mg/kg rhASA led to a reduction of the increased stride length variation to near normal values (Figure 5e). When the values measured at the four different conditions were combined, mock-treated ASA knockout mice showed significantly increased standard deviations of stride lengths for all paws ($P < 0.01$ or 0.05). High-dose-treated ASA knockout mice displayed a significantly decreased standard deviations of the left hind paw stride length in comparison to mock-treated controls ($P < 0.05$). For the other paws strong trends for reduced variation were detectable.

The correlation of left front/hind distance to right front/hind distance was taken as a second and independent measure for the uniformity of the gait. The correlation coefficient is high if the distance between the print of the left front paw and the following placement of the left hind paw is very similar to the analogous distance between the right front and hind paw prints. As a consequence of their gait abnormalities, most combinations of velocity and slope revealed decreased correlation values for mock-treated ASA knockout mice compared to wild-type controls (Table 1). Treatment with 50 mg/kg led to an increase of all correlation coefficients. In contrast to high-dose treatment, no clear effect of low-dose treatment was detectable at any condition.

Mock-treated ASA knockout mice swam significantly slower than wild-type controls (Figure 5f, $P < 0.01$). On average, the velocity of mock-treated ASA knockout mice was reduced by 26%. The mean velocity was increased by 6 and 20% after low- and high-dose treatment, respectively. The difference between mock-treated and high-dose-treated ASA knockout mice was at the edge of statistical significance ($P = 0.05$).

DISCUSSION

We have shown in a previous proof-of-concept study that short-term ERT of conventional ASA knockout mice with a dose of 20 mg/kg rhASA improves the nervous system histopathology and function.¹³ In these trials the number of injections was limited to four because mice developed a strong immunological response to the rhASA. In the present study we used immunotolerant mice that allow to assess the benefits of long-term treatment. In addition, to reveal possible dose-dependent effects, we chose to treat young presymptomatic mice with two clearly distinct enzyme doses of 4 and 50 mg/kg body weight two times a week for 26 weeks, respectively.

As determined by TLC, treatment with 50 mg rhASA/kg led to a substantial reduction of excess sulfatide in all tissues analyzed (Figure 1). Most important, sulfatide storage was reduced by up

to 84% in the PNS and by up to 45% in the CNS. The profound response of the nervous system, the major site of disease in MLD, confirms the main results of our previous study.¹³ During the entire treatment period of the present study, high-dose-treated animals received a more than 30-fold higher cumulative enzyme dose than mice of the previous short-term study. Despite the clear difference between the cumulative doses, the extent of storage reduction in the nervous system was, however, almost the same. Thus, excess sulfatide of sciatic nerve, plexus brachialis, and brain was diminished by 84, 63, and 34%, respectively, in the present, and by 82, 65, and 30%, respectively, in the previous study.¹³ Although the mouse strains, mouse ages, and enzyme batches were different, the consistency of the data suggests that the extent of storage reduction might be limited and that the upper limit has already been achieved upon four injections of 20 mg/kg. A critical threshold above which an increase of the enzyme dose or treatment duration does not further enhance therapeutic effects has been recognized in other ERT approaches as well. In acid α -glucosidase knockout mice, which reproduce the muscle phenotype of human Pompe disease, for example, neither an increase of enzyme doses from 20 to 100 mg/kg nor a prolongation of treatment from 12 to 24 weeks augmented the limited response of skeletal muscles.^{7,23} This was ascribed to a very low expression of MPR300, clathrin, and adaptor protein AP-2 in type II myofibers preventing efficient enzyme uptake by this particular cell type. Cells with a low ability to endocytose lysosomal enzymes may also exist in other tissues and delimit therapeutic efficacy of ERT in ASA knockout mice.

This view is supported by the histological analysis of enzyme-treated animals that revealed substantial regional and cell type-specific differences in sulfatide clearance. Such differences can be most clearly seen in kidney, where epithelial cells of different nephron segments, although being in immediate spatial vicinity, responded differentially to treatment. Thus, storage was reduced in descending thin limb, but not in TAL (Figure 2d,e). Clearly it would be of interest to analyze the cell type-specific expression levels of MPR300 and other components of the M6P-dependent endocytic pathway and to relate them to the differential response of these cells to therapy. Analyses of the pretreatment histology in 1–2-month-old mice (not shown) indicated that storage of TAL did not only persist, but increase during treatment. This suggests that enzyme uptake by cells of the TAL might be too low to allow even for a partial compensation of the catabolic defect. Regarding substrate clearance from the CNS, the BBB is believed to be the major limiting factor. Despite the BBB, an improvement of the CNS histopathology was achieved in ASA knockout mice (Figure 3). However, similar to kidney, regional differences were also obvious in the CNS. Thus, the potential of high-dose ERT to prevent sulfatide accumulation declined in the order hippocampal fimbria, spinal cord, and brain stem. The identification of enzymatic and cellular factors guiding the pattern of storage reduction and persistence in the CNS might be crucial for future improvements of ERT.

Lowering the enzyme dose from 50 to 4 mg/kg clearly diminished the extent of storage reduction in all tissues under investigation. In kidney and sciatic nerve, for example, 1.7- and 2.5-fold less excess sulfatide disappeared (Figure 1a). In contrast to peripheral tissues, low-dose treatment was without effect on sulfatide levels

in spinal cord and brain (Figure 1d,e). It is conspicuous that the CNS response of all preclinical ERT studies in which clearance of brain storage has been observed so far (aspartylglucosaminuria, α -mannosidosis, MPS VII, MLD) strictly depended on higher enzyme doses.^{9–12} In β -glucuronidase-deficient mice, for example, four injections of 20 mg/kg β -glucuronidase, but not three injections of 5 mg/kg reduced glial and neuronal storage. The requirement of higher doses has been ascribed to the paucity of receptors mediating transcytosis of lysosomal enzymes across the BBB and the abundance of receptors in the periphery that compete for enzyme binding.^{24,25} Consequently, saturation of the peripheral receptors, for example, by soluble M6P (MPRs) or mannan (mannose receptors) might be an option to increase CNS transfer of therapeutic enzyme.

ASA knockout mice display only minor deficits in more conventional behavioral tests before the second year of age.^{21,22} This and a previous report, however, demonstrate signs of ataxia in different measures of gait and motor coordination in 6–7-month-old mice that are reminiscent of first clinical signs in MLD (Figure 5;²⁶). Treatment with 4 or 50 mg/kg rhASA led to a consistent improvement of all neuromotor deficits, as errors in treadmill walking and alterations in stride lengths of ASA knockout mice were virtually normalized already after low-dose treatment (Figure 5a–e). Because low-dose treatment had a clear effect on sulfatide storage in the PNS, but was ineffective in reducing CNS storage (Figure 1d,e), the corrective effect with both enzyme doses may reflect improvements in the PNS function only. ASA-deficient knockout mice, however, do not demyelinate, and it is unclear to what extent CNS storage contributes to motor deficits in the animals. If the contribution of CNS storage to motor deficits is negligible, functional improvements as a result of therapeutic effects on brain cannot be expected in this mouse model. Therefore, it cannot be definitely excluded from the data presented here that low-dose treatment has no positive functional consequences for the CNS in mice or MLD patients.

Positive effects on neuromotor deficits of ASA knockout mice were also seen in recent gene therapy approaches.^{27–32} In an *in vivo* gene therapy trial an adeno-associated virus conferring hASA overexpression was injected into the brains of ASA-deficient mice.^{27,28} Treatment led to eightfold increased hASA levels compared to hASA levels of normal human brain. In accordance with these supranormal enzyme levels, the study could demonstrate a partial normalization of the sulfatide/galactosylceramide ratio in the brain, an almost complete reduction of sulfatide storage and an improvement of neuromotor deficits. Two *ex vivo* gene therapy studies employed transplantation of hematopoietic stem cells that were genetically modified to overexpress hASA.^{29–32} Although the same ASA knockout strain and hASA cDNA was used, the results of the two trials were divergent. Although one study achieved up to 33% of the normal ASA activity in brain, with no significant improvement of biochemical and pathological findings,^{29,30} the other study achieved only 10% of normal activity and substantial improvements.^{31,32} Unfortunately, the latter study did not quantify the reduction of sulfatide in brain, so that it is difficult to compare the various therapeutic attempts. The comparison is further complicated by conflicting data about the pathology of untreated control mice. Thus, Biffi *et al.* reported demyelination and severely

reduced nerve conduction velocity in 12-month-old mice (and a complete correction of both parameters after treatment).^{31,32} None of the other groups, however, did so far find any evidence for demyelination^{17,20,30} and reduced nerve conduction velocity (U. Matzner, unpublished results) in untreated ASA knockout mice up to 24 months of age. To demonstrate possible therapeutic effects of ERT and other therapy approaches on these parameters comparable studies must, therefore, be performed in demyelinating ASA-deficient mice that were generated recently.³³ The preclinical data presented here, however, indicate that enzyme doses of 4 mg/kg might already be appropriate to ameliorate PNS pathology and higher enzyme doses are required to target the CNS disease. Thus, doses of 20–50 mg/kg reduce, but do not prevent lipid storage in brain and spinal cord. It is certainly worthwhile to determine the dose necessary to elicit CNS effects more precisely because this could provide important information for future clinical studies.

MATERIALS AND METHODS

Mice and treatment. ASA knockout mice that were immunotolerant to human ASA and age-matched wild-type mice of the mixed genetic background (129ola \times C75Bl6) were used throughout this study.¹⁵ Animals were maintained on a 12-hour-light and 12-hour-dark schedule with *ad libitum* access to food and water. Handling and treatment of mice was approved by the local authorities (Permit no. 50.2032-BN24 1/05; Bezirksregierung Köln, Cologne, Germany) and consistent with the federal guidelines. Mice were 6–7 weeks old at start of treatment. Human ASA was produced in Chinese hamster ovary cells according to previously established protocols.¹³ Treatment and processing of mice for histological and biochemical analyses was as described.¹³

Hematological and urinary investigations. Hematological measurements were made with the full blood-count analyzer Advia 120 (Bayer Diagnostics Europe, Dublin, Ireland) and the hemostasis analyzer AMAX Destiny (Trinity Biotech, Lemgo, Germany). Laboratory investigation for clinical chemistry was made with a KONELAB 20i (LabSystems Clinical Laboratory Division, Espoo, Finland). Specific gravity of urine was analyzed with an Atago Refractometer (Honcho; Itabashi-ku, Tokyo, Japan) and analyte concentrations were measured using the Combur 10 test (Roche, Basel, Switzerland).

Biochemical analyses. Lipid profiles of tissues were analyzed by TLC as described.¹³

Histological analyses. Kidneys, cervical spinal cord, brain, and cochleae were dissected out from mice fixed by perfusion with glutaraldehyde. For the detection of sulfatide storage, tissue slices (100 μ m) were prepared with a vibratome and incubated with alcian blue as previously described.^{13,17} It is important to mention that the incubation conditions (pH 5.7, 300 mmol/l MgCl₂) were appropriate to yield selective staining of sulfatides. Furthermore, tissue blocks of brain tissue and cochleae (after demineralization with EDTA) were incubated with alcian blue prior to embedding in paraffin for preparing 5 μ m sections. In addition, kidney samples postfixed with OsO₄ were embedded in epoxy-resin according to standard methods and semithin sections were stained with toluidine blue. Cryostat sections of kidney were stained with alcian blue at pH 1.

The ganglion cell density in the spiral ganglion was determined by visual inspection of sections through the basal turn of the left cochlea. Number of ganglion cells were counted in semithin sections within test areas of 100 \times 100 μ m². For each mouse, ganglion cell densities of four parallel sections were averaged. Alcianophilic profiles in the cervical spinal cord and hippocampal fimbria were counted using the image

processing and analysis software, Image J (<http://rsb.info.nih.gov/ij/>), essentially as described.¹³ Briefly, storage profiles were counted in four nonoverlapping test areas (200 × 200 μm² each) of representative sections through relevant regions. The four counts per section were averaged and the values were used for the calculation of the indicated arithmetic means and SDs of experimental groups (Figure 4a,b). Statistical analysis was done by unpaired Student's *t*-test using InStat version 3.06 (GraphPad, San Diego, CA). *P* < 0.05 was considered statistically significant.

Behavioral analyses. Walking endurance and gait patterns were analyzed using a motor-driven treadmill essentially as described.²⁶ Mice were acclimated to treadmill running three times before the actual experiment was done. During the training phase the belt was positioned at a slope of 5° and adjusted to a constant velocity of 19 cm/s. Mice were encouraged to keep pace with the treadmill using an electric grid placed at the end of the treadmill (1.5 mA, 200 ms pulses, 4 Hz). A training trial was terminated when a mouse received a second electric foot shock. The challenge phase consisted of four consecutive trials, each with a different combination of slope and speed (16 cm/s 0°, 16 cm/s 10°, 22 cm/s 0°, 22 cm/s 10°). Mice stayed on the treadmill for a fixed period of 60 s. During this time, the total number of foot shocks was recorded.

In addition, mice were filmed with a digital video camera that was placed below the transparent treadmill belt. The images were used to reconstruct the gait pattern and parameters were extracted to summarize the gait characteristics of each mouse. Data on stride length (distance between two subsequential prints of the same paw) and front/hind distance (distance between a front paw and the following placement of the ipsilateral hind paw) were obtained using an automated algorithm. Standard deviations of these parameters and correlations between analogous parameters were calculated as indicators of gait uniformity.

For the determination of the swimming velocity, mice were placed at a defined starting point in a circular pool (diameter 150 cm) filled with water (26°C), which was opacified with nontoxic white paint. Swimming paths were recorded for 100 seconds using the EthoVision video tracking equipment (Noldus Bv, Wageningen, The Netherlands). The software allowed for the calculation of the mean swimming velocity and other swimming parameters.

ACKNOWLEDGMENTS

This work was supported by the European Leukodystrophy Foundation (ELA). We declare the following conflict of interest: Recombinant enzyme (human ASA) used in this study and an ongoing phase I/II clinical trial has been produced by Zymenex A/S. C.W., C.A., and C.E. are salaried employees of Zymenex. J.F. is president and chief executive officer of Zymenex.

REFERENCES

- Kornfeld, S and Mellman, I (1989). The biogenesis of lysosomes. *Annu Rev Cell Biol* **5**: 483–525.
- Brady, RO and Schiffmann, R (2004). Enzyme-replacement therapy for metabolic storage disorders. *Lancet Neurol* **3**: 752–756.
- Matzner, U, Matthes, F, Weigelt, C, Andersson, C, Eistrup, C, Fogh, J *et al.* (2008). Non-inhibitory antibodies impede lysosomal storage reduction during enzyme replacement therapy of a lysosomal storage disease. *J Mol Med* **86**: 433–442.
- Wang, J, Lozier, J, Johnson, G, Kirshner, S, Verthelyi, D, Pariser, A *et al.* (2008). Neutralizing antibodies to therapeutic enzymes: considerations for testing, prevention and treatment. *Nat Biotechnol* **26**: 901–908.
- Walkley, SU (2003). Neurobiology and cellular pathogenesis of glycolipid storage diseases. *Philos Trans R Soc Lond B Biol Sci* **358**: 893–904.
- Hollak, CE, Vedder, AC, Linthorst, GE and Aerts, JM (2007). Novel therapeutic targets for the treatment of Fabry disease. *Expert Opin Ther Targets* **11**: 821–833.
- Raben, N, Danon, M, Gilbert, AL, Dwivedi, S, Collins, B *et al.* (2003). Enzyme replacement therapy in the mouse model of Pompe disease. *Mol Genet Metab* **80**: 159–169.
- Prows, CA, Sanchez, N, Daugherty, C and Grabowski, GA (1997). Gaucher disease: enzyme therapy in the acute neuronopathic variant. *Am J Med Genet* **71**: 16–21.
- Dunder, U, Kaartinen, V, Valtonen, P, Väänänen, E, Kosma, VM, Heisterkamp, N *et al.* (2000). Enzyme replacement therapy in a mouse model of aspartylglycosaminuria. *FASEB J* **14**: 361–367.
- Roces, DP, Lüllmann-Rauch, R, Peng, J, Balducci, C, Andersson, C, Tollersrud, O *et al.* (2004). Efficacy of enzyme replacement therapy in alpha-mannosidosis mice: a preclinical animal study. *Hum Mol Genet* **13**: 1979–1988.
- Blanz, J, Stroobants, S, Lüllmann-Rauch, R, Morelle, W, Lüdemann, M, D'Hooge, R *et al.* (2008). Reversal of peripheral and central neural storage and ataxia after recombinant enzyme replacement therapy in alpha-mannosidosis mice. *Hum Mol Genet* **17**: 3437–3445.
- Vogler, C, Levy, B, Grubb, JH, Galvin, N, Tan, Y, Kakkis, E *et al.* (2005). Overcoming the blood-brain barrier with high-dose enzyme replacement therapy in murine mucopolysaccharidosis VII. *Proc Natl Acad Sci USA* **102**: 14777–14782.
- Matzner, U, Herbst, E, Hedayati, KK, Lüllmann-Rauch, R, Wessig, C, Schröder, S *et al.* (2005). Enzyme replacement improves nervous system pathology and function in a mouse model for metachromatic leukodystrophy. *Hum Mol Genet* **14**: 1139–1152.
- von Figura, K, Gieselmann, V and Jaeken, J (2001). Metachromatic leukodystrophy. In: Scriver, CR, Beaudet, AL, Sly, WS, Valle, D, Childs, B, Kinzler, KW, Vogelstein, B (eds). *The Metabolic and Molecular Bases of Inherited Disease*. Mc Graw-Hill: New York, pp. 3695–3724.
- Matzner, U, Matthes, F, Herbst, E, Lüllmann-Rauch, R, Callaerts-Vegh, Z, D'Hooge, R *et al.* (2007). Induction of tolerance to human arylsulfatase A in a mouse model of metachromatic leukodystrophy. *Mol Med* **13**: 471–479.
- Lüllmann-Rauch, R, Matzner, U, Franken, S, Hartmann, D and Gieselmann, V (2001). Lysosomal sulfoglycolipid storage in the kidneys of mice deficient for arylsulfatase A (ASA) and of double-knockout mice deficient for ASA and galactosylceramide synthase. *Histochem Cell Biol* **116**: 161–169.
- Wittke, D, Hartmann, D, Gieselmann, V and Lüllmann-Rauch, R (2004). Lysosomal sulfatide storage in the brain of arylsulfatase A-deficient mice: cellular alterations and topographic distribution. *Acta Neuropathol* **108**: 261–271.
- D'Hooge, R, Coenen, R, Gieselmann, V, Lüllmann-Rauch, R and De Deyn, PP (1999). Decline in brainstem auditory-evoked potentials coincides with loss of spiral ganglion cells in arylsulfatase A-deficient mice. *Brain Res* **847**: 352–356.
- Coenen, R, Gieselmann, V and Lüllmann-Rauch, R (2001). Morphological alterations in the inner ear of the arylsulfatase A-deficient mouse. *Acta Neuropathol* **101**: 491–498.
- Hess, B, Saftig, P, Hartmann, D, Coenen, R, Lüllmann-Rauch, R, Goebel, HH *et al.* (1996). Phenotype of arylsulfatase A-deficient mice: relationship to human metachromatic leukodystrophy. *Proc Natl Acad Sci USA* **93**: 14821–14826.
- D'Hooge, R, Hartmann, D, Manil, J, Colin, F, Gieselmann, V and De Deyn, PP (1999). Neuromotor alterations and cerebellar deficits in aged arylsulfatase A-deficient transgenic mice. *Neurosci Lett* **273**: 93–96.
- D'Hooge, R, Van Dam, D, Franck, F, Gieselmann, V and De Deyn, PP (2001). Hyperactivity, neuromotor defects, and impaired learning and memory in a mouse model for metachromatic leukodystrophy. *Brain Res* **907**: 35–43.
- Raben, N, Fukuda, T, Gilbert, AL, de Jong, D, Thurberg, BL, Mattaliano, RJ *et al.* (2005). Replacing acid alpha-glucosidase in Pompe disease: recombinant and transgenic enzymes are equipotent, but neither completely clears glycogen from type II muscle fibers. *Mol Ther* **11**: 48–56.
- Urayama, A, Grubb, JH, Sly, WS and Banks, WA (2004). Developmentally regulated mannose 6-phosphate receptor-mediated transport of a lysosomal enzyme across the blood-brain barrier. *Proc Natl Acad Sci USA* **101**: 12658–12663.
- Urayama, A, Grubb, JH, Banks, WA and Sly, WS (2007). Epinephrine enhances lysosomal enzyme delivery across the blood brain barrier by up-regulation of the mannose 6-phosphate receptor. *Proc Natl Acad Sci USA* **104**: 12873–12878.
- Stroobants, S, Leroy, T, Eckhardt, M, Aerts, JM, Berckmans, D and D'Hooge, R (2008). Early signs of neuropiloidosis-related behavioral alterations in a murine model of metachromatic leukodystrophy. *Behav Brain Res* **189**: 306–316.
- Sevin, C, Benraiss, A, Van Dam, D, Bonnin, D, Nagels, G, Verot, L *et al.* (2006). Intracerebral adeno-associated virus-mediated gene transfer in rapidly progressive forms of metachromatic leukodystrophy. *Hum Mol Genet* **15**: 53–64.
- Sevin, C, Verot, L, Benraiss, A, Van Dam, D, Bonnin, D, Nagels, G *et al.* (2007). Partial cure of established disease in an animal model of metachromatic leukodystrophy after intracerebral adeno-associated virus-mediated gene transfer. *Gene Ther* **14**: 405–414.
- Matzner, U, Harzer, K, Learish, RD, Barranger, JA and Gieselmann, V (2000). Long-term expression and transfer of arylsulfatase A into brain of arylsulfatase A-deficient mice transplanted with bone marrow expressing the arylsulfatase A cDNA from a retroviral vector. *Gene Ther* **7**: 1250–1257.
- Matzner, U, Hartmann, D, Lüllmann-Rauch, R, Coenen, R, Rothert, F, Månsson, JE *et al.* (2002). Bone marrow stem cell-based gene transfer in a mouse model for metachromatic leukodystrophy: effects on visceral and nervous system disease manifestations. *Gene Ther* **9**: 53–63.
- Biffi, A, De Palma, M, Quattrini, A, Del Carro, U, Amadio, S, Visigalli, I *et al.* (2004). Correction of metachromatic leukodystrophy in the mouse model by transplantation of genetically modified hematopoietic stem cells. *J Clin Invest* **113**: 1118–1129.
- Biffi, A, Capotondo, A, Fasano, S, del Carro, U, Marchesini, S, Azuma, H *et al.* (2006). Gene therapy of metachromatic leukodystrophy reverses neurological damage and deficits in mice. *J Clin Invest* **116**: 3070–3082.
- Ramakrishnan, H, Hedayati, KK, Lüllmann-Rauch, R, Wessig, C, Fewou, SN, Maier, H *et al.* (2007). Increasing sulfatide synthesis in myelin-forming cells of arylsulfatase A-deficient mice causes demyelination and neurological symptoms reminiscent of human metachromatic leukodystrophy. *J Neurosci* **27**: 9482–9490.